Photoelectron holography in strong optical and dc electric fields

2014 J. Phys.: Conf. Ser. 488 012007

(http://iopscience.iop.org/1742-6596/488/1/012007)

XXVIII International Conference on Photonic, Electronic and Atomic Collisions (ICPEAC 2013) IOP Publishing
Journal of Physics: Conference Series **488** (2014) 012007 doi:10.1088/1742-6596/488/1/012007

Photoelectron holography in strong optical and dc electric fields

Aneta Stodolna[1], Ymkje Huismans[1], Arnaud Rouzée[2], Franck Lépine[3] and Marc JJ Vrakking[2]

[1] FOM Insititute AMOLF, Science Park 102, 1098 XG Amsterdam, The Netherlands
[2] Max-Born-Institute (MBI), Max-Born Strasse 2A, 12489 Berlin, Germany
[3] Institut Lumière Matière, Université Lyon 1, CNRS, UMR 5306, 10 Rue Ada Byron, 69622 Villeurbanne Cedex, France

E-mail: marc.vrakking@mbi-berlin.de

Abstract. The application of velocity map imaging for the detection of photoelectrons resulting from atomic or molecular ionization allows the observation of interferometric, and in some cases holographic structures that contain detailed information on the target from which the photoelecrons are extracted. In this contribution we present three recent examples of the use of photoelectron velocity map imaging in experiments where atoms are exposed to strong optical and dc electric fields. We discuss (i) observations of the nodal structure of Stark states of hydrogen measured in a dc electric field, (ii) mid-infrared strong-field ionization of metastable Xe atoms and (iii) the reconstruction of helium electronic wavepackets in an attosecond pump-probe experiment. In each case, the interference between direct and indirect electron pathways, reminiscent of the *reference* and *signal* waves in holography, is seen to play an important role.

1. Introduction

The principle of holography was conceived in 1948 by Gabor as a method to overcome the limitations that existed in electron microscopes [1]. At the time, these instruments already provided a resolution that was far superior to that of optical microscopes, but still substantially worse than the resolution that one might hope for on the basis of the electron de Broglie wavelength. Gabor realized that holography, using the interference between a *reference* and a *signal* wave, might be able to overcome the existing limitations, and might lead - for the first time - to atomic-scale imaging. Still, lacking adequate coherent electron sources, the first electron holography experiment took many years to develop, and holography became widely known as an optical technique before it was first applied to electrons.

In the last few years, a novel interest has emerged in the application of holographic principles in atomic and molecular physics, as a result of the development of several new sources of ultrashort XUV/X-ray pulses (both free electron lasers and high-harmonic generation sources). Beside the immediate possibilities of holographic imaging using the XUV/X-ray photons [2], these sources can remove energetic electrons from atomic and molecular systems, which may be detected in attosecond pump-probe experiments on time-resolved electron dynamics or in femtosecond pump-probe experiments on time-resolved molecular dynamics. In both cases, strong indications for the possible use of holographic principles has already been given in the literature [3][4]. Furthermore, photoelectron holography plays an important role in experiments

on photoionization near threshold in dc electric fields, as will be demonstrated here [5], and in strong field ionization in mid infrared laser fields [6].

Holography, whether implemented for photons or for electrons, relies on the interference on a detector between two waves originating from a common source. One of the two waves, the *signal* wave, encounters a scattering object while travelling from the source to the detector, whereas the other (i.e. *reference*) wave travels directly from the source to the detector without experiencing a scattering event. On the detector, a destructive or constructive interference occurs, depending on the phase difference between the *signal* and *reference* wave. The interference occurs because on the detector one is unable to determine whether one is dealing with a photon/electron that travelled along the *signal* path or one that travelled along the *reference* path. Holography poses restrictions on the coherence of the photon/electron source, since the holographic interference should not depend on the position within a finite source where the photon/electron is emitted. Therefore holography using lasers preceded the application of electron holography.

When considering photoelectron emission from an atom or molecule, in the absence of couplings leading to decoherence, the coherence requirements for holography are almost automatically fulfilled. Correspondingly, when using laser ionization, the conditions for the generation of a hologram are easily realized. A crucial element remains, of course, the requirement that both a *signal* and *reference* wave can be distinguished, which do/do not interact with the parent ion before reaching the detection system. In all experiments to be discussed below, the detection system will consist of a two-dimensional microchannel plate detector, followed by a phosphor screen and a CCD camera system. Use of such a detector allows observation of the holographic interference on a very large number of distinguishable detector positions, which resolve the final momentum of the outgoing photoelectron.

2. Photoionization in a DC electric field

A first example of holography involving the interference between direct and indirect trajectories was observed in our laboratory a little over a decade ago in experiments studying the photoionization of Xe atoms near threshold in a dc electric field (typ. 500 V/cm) [7]. In the experiments metastable Xe atoms were photoionized using a tunable, narrowband dye laser, exciting the atom to energies between the saddle-point in the Coulomb + dc field potential (E_{sp} = $6.1\sqrt{F(V/cm)}$ cm $^{-1}$) and the field-free ionization limit. The resulting photoelectrons were detected on a 2D detector positioned at a distance of appr. 50 cm. In the photoionization, *reference* (direct) electron trajectories can then be distinguished where the electron is initially ejected in the down-field direction, as well as *signal* (indirect) trajectories, where the electron is initially ejected in the up-field direction. Along these *signal* trajectories the electron may interact with the ion a number of times before finding the hole in the Coulomb + dc field potential. Formulated more precisely, for each total energy an angle β_0 with respect to the electric field separates the simple, direct trajectories from the more complex, indirect trajectories [8]. Beyond an angle β_c in the upfield direction the trajectories remain classically bound.

Since there is nothing to disturb the coherence between both (direct and indirect) classes of photoelectrons, they will interfere on the detector. These interferences can be observed when the images on the detector are magnified by an order of magnitude by placing an Einzel lens between the laser interaction region and the 2D detector [9]. In Xe, all observed interferences could be understood in terms of a path integral formalism that considers the phase accumulation by the electron along different direct and indirect trajectories that connect the position of the atom to a particular location on the detector [10]. In the experiment, interferences could be separately observed for the direct and the indirect trajectories, and a beating pattern could be observed between them in regions of overlap. Though not further analyzed or discussed at the time in those terms, this may be regarded a first example of holography in our discussion.

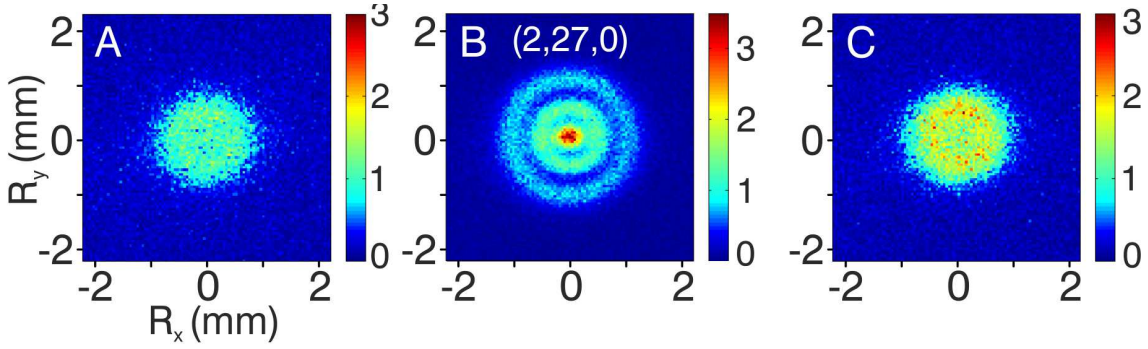

Photoionization of hydrogen atoms in an 808 V/cm dc electric field, in the energy range between the saddle-point in the Coulomb+dc potential and the field-free ionization limit. A comparison is shown between a measurement carried out for the (n_1, n_2, m) = (2, 27, 0) resonance (b) and two non-resonant measurements performed 1.8 cm^{-1} below (a) and 1.1 cm^{-1} above (c) this resonance. See [5].

While the path integral description above is fully adequate for evaluating the phase accumulation in the continuum in the case of non-resonant ionization, a special situation can arise when the photoionization first involves the excitation of a quasi-bound state. Such resonances are commonplace in the afore-mentioned energy region between the saddle-point in the Coulomb + dc electric field potential and the field-free ionization limit, and are due to the persistence of Rydberg states, which fan out into Stark manifolds. Disappointingly, hardly any modification of the interference patterns could be observed in these early Xe experiments following the excitation of quasi-bound Stark states. The reason for this are extensive perturbations described by large quantum defects. Observation of the nodal structure of quasi-bound Stark states requires that the experiments are performed for few- or ideally single-electron atoms where quantum defects are small. This feat that has only recently been accomplished in a series of experiments performed on lithium [11], helium [12] and hydrogen atoms [5]. Among these, hydrogen provides the most compelling case, because of the complete separability of the Hamiltonian in terms of parabolic coordinates ξ= r+z and η= r-z, where r is the distance of the electron from the hydrogen nucleus, and z is the displacement along the electric field axis. The electronic wavefunction can be written as a product of two wavefunctions that separately describe the dependence on ξ and η. Remarkably, the separation constant that describes the available energy for the motion along the ξ and η coordinates, is *independent* of the strength of the dc electric field, leading to the unique situation that the nodal structure of the bound wavefunction along the ξ-coordinate stays intact all the way from the point-of-ionization to the 2D detector, which as before was placed approximately 50 cm away. On the 2D detector, the quantization along the ξ-coordinate characterized by the n_1 parabolic quantum number can therefore be directly observed (see Figure 1), representing the first-ever observation of the nodal structure of hydrogen atomic wavefunctions.

More recently, we have extended these experiments to helium [12]. Helium represents an intriguing intermediate case, since it is a two-electron atom, where however, in the metastable initial state used in the experiment and in the auto-ionizing Stark state that is excited from there, one of the two electrons is very strongly bound. Like in the hydrogen experiment, interference patterns were measured for a large number of resonances corresponding to quasi-bound Stark states. Remarkably, the behaviour was hydrogen-like for some of the resonances, where a nodal structure revealing the n_1 parabolic quantum number could be inferred, whereas on other resonances it did not at all reflect the known parabolic quantum number of the resonance involved, and instead could be understood - like in the case of Xe - on the basis of path integral arguments considering the phase accumulation of the electron in the continuum. The helium results will be the subject of an upcoming publication [12].

3. Photoionization in a strong mid-infrared laser field

In the example discussed above, the *reference* and *signal* trajectories occurred in the presence of a dc electric field, and the photo-excitation (using a narrowband, nanosecond laser) was fully perturbative. However, we may expect similar trajectories to be relevant in ionization in intense laser fields, in particular when performed in the quasi-static regime, i.e. under conditions where the ionization takes place by tunneling through the Coulomb + laser electric field potential, on a time-scale that is short compared to the laser optical period. The electron then escapes the atom/molecule along the laser polarization axis and is subsequently accelerated by the laser electric field to high electron kinetic energies. Given the oscillatory nature of the laser electric field, the initial acceleration away from the ion is followed by an acceleration back towards the ion, setting the stage for laser-driven electron-ion recollisions, which are responsible for high-harmonic generation and the formation of attosecond laser pulses [13]. Besides looking for the production of XUV harmonics as a result of the re-collision, the laser-driven electron itself may also be detected, thereby revealing the occurrence of above-threshold ionization and the formation of high kinetic energies as a result of the electron momentum reversal that may occur during the re-collision. The possibility to observe holograms can be anticipated by regarding the outer turning point of the laser-driven oscillatory electron motion as an electron source. From this source the electron can reach an electron detector without re-encountering the ion along the way, moving along what we might call a *reference* trajectory, or it can - strongly under the influence of the laser field - first re-collide with the ion, and reach the detector along a *signal* trajectory. Importantly, on the detector one is unable to determine whether the electron arrived via a *signal* or *reference* trajectory, and these two pathways gives rise to an interference pattern that can be seen as a hologram of the atomic potential.

The scenario sketched above is expected to be particularly relevant in strong field ionization by long-wavelength lasers, where the outer turning point of the electron motion is far removed from the ion, i.e. at a distance where the Coulomb interaction becomes negligibly weak. Experimentally, the first observation of these photoelectron holograms was obtained in strong-field ionization of metastable Xe atoms using 4-40 μm laser pulses obtained from the FELICE intra-cavity free electron laser in Rijnhuizen, the Netherlands. Figure 2(a) shows a representative photoelectron momentum map [6]. It shows that the photoelectron angular distribution peaks along the polarization axis of the free electron laser (horizontal), and contains a number of secondary maxima away from the polarization axis. The holographic nature of these secondary maxima was proven by two theoretical methods, both relying on the Strong Field Approximation (SFA), namely the generalized Strong Field Approximation (gSFA, see [6]) and the Coulomb-Corrected Strong Field Approximation (CCSFA) [14]. In the latter method, SFA is implemented, making use of a saddle-point analysis and calculating the wavefunction amplitude at a given final momentum as a coherent sum involving a number of electron trajectories, which start out in complex time (accounting for the tunneling process) and subsequently propagate in real time (accounting for the propagation in the continuum under influence of the laser field). The Coulomb correction is readily applied by including the Coulomb interaction in the equations of motion during the real time propagation. Representative trajectories are shown in figure 2(b). This calculation shows that the holographic interference predominantly arises between two trajectories that for the chosen laser parameters (λ=7μm, I_{laser}=7x10^{11} W/cm^2) initially displace the electron by about 150 a.u. towards the right. This point, subsequently, acts as an electron source. In the region where oscillatory angular distributions are observed, the hologram is caused by an interference between red *reference* trajectories, where the laser pushes the electron back towards the left and the electron performs a laser-driven oscillatory motion without however re-encountering the ion, and blue *signal* trajectories, where the laser pushes the electron back to the left and induces an electron-ion recollision that reverses the electron momentum perpendicular to the laser polarization axis (from upwards to downwards in the

present case), so that its final momentum becomes identical to that of the red trajectory. Using the gSFA method, analytical expressions could be derived that demonstrate that the holographic pattern contains, besides spatial information, also time information (see SOM of [6]).

Since obtaining the results published in [6], we have established criteria for the observation of the holographic interference pattern [15]. Based on experiments performed between 600-800 and 1200-1600 nm, and based on calculations between 400 and 4560 nm, we have empirically determined that the observation of the holographic pattern requires that the so-called ponderomotive energy U_p (i.e. the energy describing the oscillation of a free electron in an intense laser field) satisfies $U_p/\omega_{laser} \geq 4$, thereby favouring conditions that commonly exist in the tunneling regime. Extending the experiments reported in [6] we have furthermore experimentally investigated the scaling of the holographic interference patterns with laser intensity and wavelength [16] [17]. The holographic patterns depend only weakly on the peak intensity of the laser, due to the fact that the ionization and recombination times (and therefore the phase difference between the *reference* and *signal* trajectories that are detected at a given final momentum, only weakly depend on the laser intensity. However, the laser wavelength has a strong influence on the holographic interference pattern, due to the fact that the dominant term in the phase difference between the *reference* and *signal* trajectories scales as $-(1/2)p_r{}^2\,(t_c\text{-}t_{0,ref})$, where p_r is the momentum perpendicular to the polarization axis, t_c is the recollision time and $t_{0,ref}$ is the time of ionization of the reference wavepacket. The second term in this expression scales linearly with the laser wavelength, and correspondingly the location of the secondary interference maxima away from the laser polarization axis scales inversely proportional with laser wavelength.

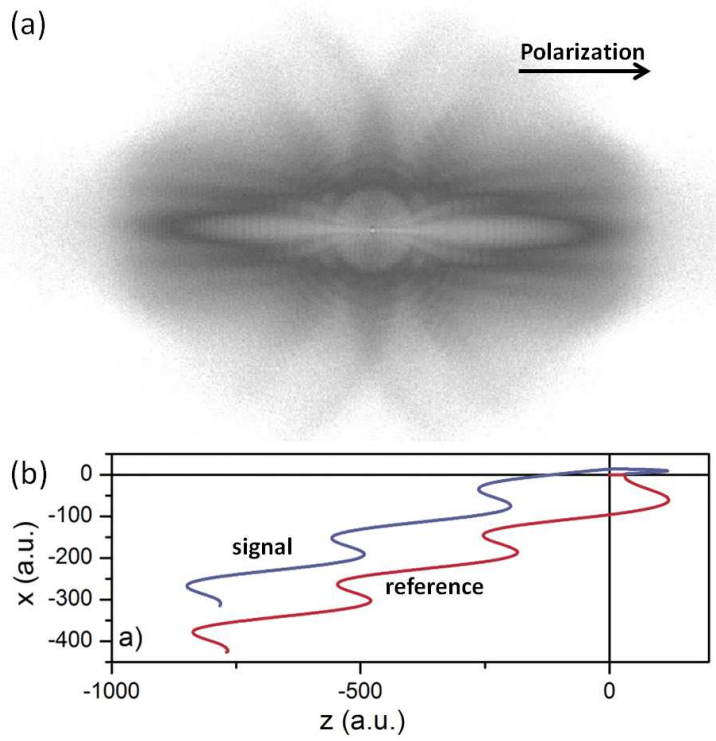

Figure 1. (a) Experimental photoelectron momentum map measured for ionization of metastable Xe atoms by 7 μm laser pulses from the FELICE free electron laser. The peak intensity of the laser was $7\text{x}10^{11}$ W/cm^2; (b) Representative electron trajectories calculated using the CCSFA method. Red trajectories perform an oscillatory motion in the laser field without re-encountering the ion, whereas blue trajectories are greatly affected by a laser-driven electron-ion recollision, which reverses the momentum of the electron transverse to the field.

Holographic interferences such as observed here for the case of mid-infrared strong field ionization are expected to be pervasive whenever (i) a clearly defined source exists (here: the outer turning point of the laser-driven electron trajectory), (ii) high energy electrons with a

small de Broglie wavelength are formed and (iii) the possibility of both *reference* and *signal* trajectories can be identified. These three criteria can also be satisfied when the ionization is performed using XUV/X-ray light. In this case inner-shell ionization localizes the electron source on a specific atom, the high photon energy provides the means to eject energetic electrons with a small de Broglie wavelength, and surrrounding atoms (in a molecule) act as potential scattering centres for the ejected electron. Indeed, measurements performed by Doerner and co-workers more than ten years ago, for core-shell photoionization of CO molecules using synchrotron radiation [18], provide clear evidence for the observation of holographic interferences, from which the internuclear distance in the molecule can be retrieved. Exploiting the novel possibilities, provided by high-harmonic and free electron lasers, to provide the pre-requisite XUV/X-ray light with a femtosecond or even attosecond pulse duration, this suggests that studies of time-dependent molecular dynamics using holographic photoelectron detection may be successfully explored [4]. This approach might present a viable alternative to present methods for studying time-resolved molecular dynamics, which rely on the availability of detailed knowledge about the relation between the structure of a molecule and its optical properties, which, however, for many systems of interest is not available. In our work we have so far tried to implement this approach using both high-harmonic and free electron laser sources. In experiments on XUV photoionization of impulsively aligned CO_2 molecules, we have managed to extract information on the orbitals of the molecule that participate in the XUV ionization process, and have seen the first hints of the evolution of the molecular frame photoelectron angular distribution with XUV photon energy (and hence, with electron kinetic energy and de Broglie wavelength) [19]. Efforts to use the method to investigate time-dependent dynamics have been most extensively pursued using the FLASH free electron laser in Hamburg, but have, due to the finite jitter between the free electron laser and the other required laser sources, so far not been possible with the pre-requisite time resolution [20].

4. Photoelectron holography on attosecond time-scales

The discussion on mid-infrared strong-field holography presented in the previous section, suggests that photoelectron holography may be used to access structural information, such as the shape of the interaction potentials that the electron experiences. However, the experiment also contains time-dependent information. If the ion undergoes time-dependent dynamics between the time of ionization and the time of the electron-ion recollision, then this dynamics may be encoded in the kinetic and angular distribution of the scattered photoelectrons, potentially allowing to track this ion dynamics on attosecond to few-femtosecond timescales. Using the formation of XUV high-harmonics as observable, such studies have already been very successfully performed for several atoms and small molecules [21] [22]. Furthermore, the holographic interference involves two trajectories which were born at slightly different times, and correspondingly the photoelectron holography experiment may provide information on the evolution of the ionization rate within the mid-IR optical cycle.

The attosecond pulses formed in the high-harmonic generation process allow the development of pump-probe spectoscopy with attosecond time-resolution, and experiments along these lines have been developed with great success in the last decade, providing first insights into electron motion in atomic, molecular and condensed phase systems on the attosecond timescale [23]. Typically, so far, attosecond pump-probe experiments are configured using the combination of an attosecond pulse (or an attosecond pulse train) and an IR laser whose optical cycle is used as a clock with attosecond time-resolution. In the pump-probe sequence, the attosecond pulse is either used to initiate the electron dynamics of interest, or to probe it.

Holographic principles can be exploited in attosecond pump-probe experiments when one is able to exploit the interference between photoelectrons (or ions) that result from the pump-probe sequence with photoelectrons (or ions) that result from a pump-only or a probe-only laser

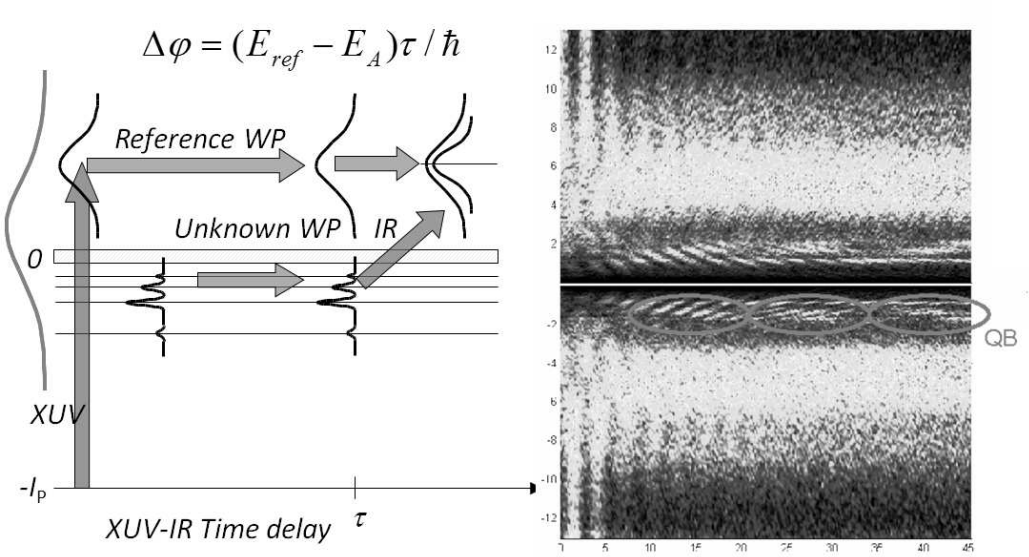

Figure 2. Attosecond time-resolve photoelectron holography using an XUV isolated attosecond pulse and a time-delayed few-cycle IR pulse. The XUV attosecond pulse produces both a Rydberg electron wavepacket and a *reference* continuum electron wavepacket. After a variable time delay, the Rydberg wavepacket is ionized by the few-cycle IR pulse, creating a *signal* electron wavepacket that interferes with the *reference* wavepacket on the detector, allowing a reconstruction of the amplitudes and relative phases of the Rydberg wavepacket. Adapted from [3]

interaction. The first example of such an experiment was performed a few years ago and allowed the holographic reconstruction of bound electron wavepackets in the helium atom [3]. In the experiment (see Figure 3), an isolated attosecond laser pulse was used to photo-excite helium, producing a Rydberg electron wavepacket. At the same time, given that part of the bandwidth of the attosecond pulse was above the helium ionization potential, a continuum electron wavepacket was formed. At a variable delay, a few-cycle IR pulse interacted with the system. Since the continuum electron wavepacket rapidly moves away from the ion, it is not affected by the IR pulse, and therefore plays the role of a *reference*. The Rydberg wavepacket is ionized by the few-cycle IR pulse, producing a *signal* continuum electron wavepacket that interferes with the former *reference* wavepacket on the detector, where one cannot know whether a detected electron arises through a pump-only (*reference*) or pump-probe (*signal*) laser interaction. By varying the pump-probe time-delay, the rate at which the phase difference between the *reference* and *signal* waves grows can be determined, allowing a determination of the energy of the bound state. In fact, although not yet fully realized in [3], the angle-, kinetic energy and time-resolved observation of the holographic pattern allows a complete reconstruction of the amplitudes and phases of the Rydberg electron wavepacket.

5. Conclusions and Outlook

As discussed in this article, the formation of holograms involving the interference between a *reference* electron wave that leaves an atomic or molecular system directly along a simple trajectory and a *signal* electron wave that involves a more complex motion (and potentially a second, time-delayed laser interaction), has in the last few years been recognized in a number of situations of dynamical interest, including both the ionization in strong optical and dc electric

fields, and particular implementations of attosecond pump-probe spectroscopy. An attractive aspect of all these holographic measurements, is that they compare the unknown properties of a *signal* wave to those of a generally better-known *reference* wave, along the way also benefitting from the fact that weak *signal* contributions can be more easily observed when they are amplified by heterodyning against a more powerful *reference* contribution. The work discussed here shows that significant work is still needed to extract all the information contained in the holograms (atomic and molecular structure, potentials and orbitals, electronic wavepacket composition, etc.), in particular in the holograms that are obtained in mid-infrared strong-field ionization.

5.1. Acknowledgments

The material presented in this paper is to a large extent based on three different experiments [5] [6] [3], each involving a large number of collaborators. In this context we would particularly like to acknowledge our fruitful collaborations with Profs. Giuseppe Sansone and Mauro Nisoli (Politecnico di Milano), Prof. Anne L'Huillier and Dr. Johan Mauritsson (Univ. of Lund), Prof. Ken Schafer (LSU), Prof. Misha Ivanov and Dr. Olga Smirnova (MBI), Prof. Dieter Bauer (Univ. of Rostock), Prof. Sergey Propuzhenko (Moscow Engineering Physics Instiute), Prof. Christian Bordas (Univ. of Lyon), Prof. Francis Robicheaux (Auburn University), Prof. Samuel Cohen (University of Ioannina), the FELICE staff, and a number of previous Phd students and postdocs in our team, in particular Dr. Freek Kelkensberg, Dr. Wing Kiu Siu, Dr. Omair Ghafur, Dr. Tatiana Martchenko, Dr. Julia Jungmann and Dr. Arjan Gijsbertsen.

5.2. References to printed journal articles

[1] Gabor B 1948 *Nature* **161** 778
[2] Chapman HN *et al* 2007 *Nature* **448** 676
[3] Mauritsson J *et al* 2010 *Phys. Rev. Lett.* **105** 053001
[4] Krasniqi F, Najjari B, Struder L, Rolles D, Voitkiv A and Ullrich J 2010 *Phys. Rev. A* **83** 033411
[5] Stodolna A, Rouzée A, Lépine F, Cohen S, Robicheaux F, Gijsbertsen A, Jungmann JH, Bordas C and Vrakking MJJ 2013 *Phys. Rev. Lett.* **110** 213001
[6] Huismans Y *et al* 2011 *Science* **331** 61
[7] Nicole C, Sluimer I, Rosca-Pruna F, Warntjes M, Vrakking M, Bordas C, Texier F and Robicheaux F 2000 *Phys. Rev. Lett.* **85** 4024
[8] Bordas C 1998 *Phys. Rev. A* **58** 400
[9] Offerhaus HL, Nicole C, Lepine F, Bordas C, Rosca-Pruna F and Vrakking MJJ 2001 *Rev. Sci. Instrum.* **72** 3245
[10] Nicole C, Offerhaus HL, Vrakking MJJ, Lepine F and Bordas C 2002 *Phys. Rev. Lett.* **88** 133001
[11] Cohen S, Harb MM, Ollagnier A, Robicheaux F, Vrakking MJJ, Barillot T, Lépine F and Bordas C 2010 *Phys. Rev. Lett.* **110** 183001
[12] Stodolna A *et al* 2013 *in preparation*
[13] Corkum PB 1993 *Phys. Rev. Lett.* **71** 1994
[14] Popruzhenko SV and Bauer D 2008 *J. Mod. Opt.* **55** 2573
[15] Marchenko T, Huismans Y, Schafer KJ and Vrakking MJJ 2010 *Phys. Rev. A* **84** 053427
[16] Huismans Y *et al* 2012 *Phys. Rev. Lett.* **109** 013002
[17] Hickstein D *et al* 2012 *Phys. Rev. Lett.* **109** 073004
[18] Landers A*et al* 2001 *Phys. Rev. Lett.* **87** e013002
[19] Kelkensberg F*et al* 2012 *Phys. Rev. A* **84** 051404(R)
[20] Rouzée A *et al* 2013 *J. Phys. B* in press
[21] Smirnova O, Mairesse Y, Patchkovskii S, Dudovich N, Villeneuve D, Corkum P and Ivanov MY 2009 *Nature* **460** 972
[22] Shafir D, Soifer H, Bruner BD, Dagan M, Mairesse Y, Patchkovskii S, Ivanov MY, Smirnova O and Dudovich N 2012 *Nature* **485** 343
[23] Krausz F and Ivanov M 2009 *Rev. Mod. Phys.* **81** 163